



When jelly gets the blues

Audible sound generation with gels and its origin

Christian Sinn *

PMS Optik AG, Kölner Straße 42, 60327 Frankfurt/Main, Germany

Received 3 September 2003; received in revised form 1 September 2004

Available online 18 October 2004

Abstract

We report investigations concerning the mechanism for the audible sound generation of humming or ringing gels. As claimed earlier, the sound stems from the resonance of shear modes within the gel body. We present evidence for this claim by comparing the directly measured sound velocity, determined with a simple acoustic spectrometer, with the calculated one from measurements of the shear modulus and the mass density. Data were collected for different gel porosities. Deviations at comparatively small porosities are assumed as due to a frequency-dependent shear modulus.

© 2004 Elsevier B.V. All rights reserved.

PACS: 62.65.+k; 43.20.Jr; 82.70.Gg

1. Introduction

For about 50 years, the sound propagation in porous media has been investigated both theoretically and experimentally, initiated by the theory developed by Biot [1], originally intended to describe the sound propagation in marine sediments. Applications ranged from submarine oil recovery to measurements of the acoustic properties of different natural porous minerals, e.g. sandstone [2]. The theory was also applied early to the description of acoustic properties of colloidal suspensions [3]. Today, the interest focuses on advanced applications, e.g., on sound modes in liquid helium confined in a porous medium [4]. A review of different regimes of Biot's theory by Johnson is available [5,6]. In addition, the excellent book by Bourbié et al. [7] deserves mention.

Earlier work by Wood [8] is relevant here as well. He gave a formula for the decrease of the sound velocity

owing to air bubbles in a liquid, e.g. in sparkling beverages.

The present contribution is devoted to gels. They consist of a more or less rigid body with a sponge-like solid structure that is filled with a liquid. For gels, Biot's theory predicts essentially three independent sound modes [5]: a compression mode very much like the usual sound propagation in a viscous liquid, however modified for the presence of the solid frame according to Wood's formula. Second, a slow-wave, the sound velocity of which is imaginary in the case of gels, corresponding to a diffusive propagation of pressure within the network. Third, a shear wave, which is overdamped in a viscous liquid where the shear modulus vanishes. If excited, it decays exponentially on a length scale δ known as viscous skin depth [9]. In gels, δ is significantly larger than the pore diameter. Accordingly, the gel liquid is efficiently fixed by viscous forces in the porous gel body.

Experimentally, these predictions have been confirmed for a wide variety of materials. For gels, the diffusive behavior of the slow-mode has been first established by Tanaka et al. [10]. They observed a diffusive mode in polymer gels and related the diffusion coefficient

* Tel.: +49 69 7500 1619; fax: +49 69 7500 1617.

E-mail address: christian.sinn@pms-optik.de

measured by dynamic light scattering to the elastic moduli of the gel body. Later, the presence of propagating compression and shear modes in gels has been established by direct measurements of the sound velocity, as well as in colloidal [11] and polymer gels [12], in aerogels [13], and their precursors [14].

A second streamline for the present investigation consists of the re-discovery of ‘ringing’ or ‘humming’ gels by Hoffmann and co-workers, investigating microemulsions of high droplet concentration. Their structural properties had been characterized extensively [15]. In addition, Oetter and Hoffmann [16] described the response of these gels to an acoustic stimulus and calculated elastic moduli from the determined sound velocity. The quantitative description of their observation, however, remained a bit vague, and the interpretation of their results with respect to the relevant elastic modulus seems even to be in contradiction to Biot’s theory, to which they do not refer in their paper. Earlier investigations of the acoustical properties of gels date back to the time of Kohlrausch (1893); systematical experiments on different factors influencing the sound pitch are reported by Holmes et al.¹ [17].

The present contribution is thought to join these streamlines by new experiments. It was motivated by the study of aerogel precursors (silica sponges filled with alkanol) as hosts for the diffusion of colloidal particles. I observed a strong humming of these highly porous structures and investigated this effect upon variation of the sample porosity.

The aim of this paper is to give evidence for my earlier claim [18] that the humming of the gel samples originates from resonances of shear waves within the gel body. For this purpose I shall start with a brief description of Biot’s theory with emphasis on its application to gels. Subsequently, I shall demonstrate that the sound velocity from the audible resonance is equal to that of the predicted shear wave, which has been determined independently from measurements of the shear modulus and the material mass density.

2. Theoretical considerations

Biot’s theory describes phenomenologically the propagation of acoustic waves in a porous, fluid-filled, macroscopically homogeneous and isotropic body. Each volume element of this body experiences an average displacement of the fluid and the solid part, respectively. The respective equations of motion are coupled by viscous, as well as inertial, forces. The macroscopic material properties that enter are the bulk moduli of the fluid (K_f) and the solid (K_s) phase, the bulk modulus

K_b of the skeletal frame, the shear modulus G , and the porosity ε . I adopted the notation of Ref. [5], to which I refer the reader for details.

General hydrodynamics predicts a crossover between two distinct regimes that is governed by the viscous skin depth, $\delta = (2\eta/\rho_f\omega)^{1/2}$ [9], with η the (shear) viscosity of the fluid phase and ρ_f its mass density, ω is the (angular) frequency of a shear disturbance, e.g. produced by two tangentially moving plates. For porous media, this crossover separates a high-frequency from a low-frequency regime, the crossover frequency $\omega_c = 2\eta/\rho_f a^2$ being related to the average pore size a of the medium. Porous materials that exhibit pore sizes of the order of 100 nm and less, like the silica gels of this study, are always in the low-frequency regime. This means that the viscous skin depth is much larger than the characteristic pore size, thus fixing the fluid by viscous forces. Furthermore, for gels the skeletal frame is generally much more compressible than the pore fluid. A ‘gel limit’ can be identified therefore by $K_b, G \ll K_f$.

Applying these considerations, the theory predicts the following sound modes in the porous medium: First, there is a fast compressional mode, which is very much alike the longitudinal sound mode in pure liquids. The sound velocity of this longitudinal mode is given by

$$c_{FL} = c_0 \left[1 + \frac{\xi_1 K_b + \xi_2 G}{2K_f} \right], \quad (1)$$

where $c_0^2 = K_m/\rho_m$ is Wood’s result [8] for the sound velocity in a composite medium with $K_b = G = 0$, for example a colloidal suspension, with mean density $\rho_m = \varepsilon\rho_f + (1 - \varepsilon)\rho_s$. The bulk modulus of the composite medium can be calculated assuming two different elastic media in parallel, yielding for our case $K_m^{-1} = \varepsilon K_f^{-1} + (1 - \varepsilon)K_s^{-1}$. The ξ_i in Eq. (1) represent the deviations from Wood’s formula due to the finite stiffness of the frame. $\xi_1 = \varepsilon^2(K_m K_f)(K_f^{-1} - K_s^{-1})^2$ and $\xi_2 = \frac{4}{3}K_f/K_m$. The sound attenuation can be calculated correspondingly. The compression mode treated so far can be visualized as a cooperative in-phase motion of fluid and skeletal frame in a distinct volume element.

Second, there exists a slow compressional mode, corresponding to the out-of-phase motion of fluid and skeleton. The sound velocity of this wave is purely imaginary,

$$c_{SL}^2 = -i\omega \frac{k(K_b + \frac{4}{3}G)}{\eta}, \quad (2)$$

corresponding to an overdamped sound mode. k is the permeability defined through Darcy’s law $Q = -(kA/\eta)\nabla p$, which relates the volume flow rate Q through a sample area A to an applied hydrostatic pressure gradient ∇p . Eq. (2) can be used to calculate elastic constants of gels from line width measurements by dynamic light scattering, as performed by Tanaka et al. [10].

¹ I thank the referee for drawing my attention to this work.

Third, there is only one trivial shear mode, corresponding to the out-of-phase movement of fluid and skeleton. The sound velocity of this transversal wave is given by

$$c_T = \left(\frac{G}{\rho_m} \right)^{1/2}. \quad (3)$$

Accordingly, for porous media in the 'gel limit', from theory one expects two propagating sound modes with different sound velocities, which are determined by Eqs. (1) and (3). Notice that both modes are non-dispersive, i.e. the sound velocity is independent of frequency.

From $G \ll K_f$, one can already estimate that the longitudinal sound velocity c_{FL} should be some orders of magnitude higher than the transversal one, c_T . I defer the straightforward calculation of the eigenmodes of a finite body to the following M^3 section. However, an educated guess unfolds that only c_T could lead to audible frequencies, whereas c_{FL} is almost always expected to generate ultrasound.

3. Materials, methods and measurements

3.1. Gel preparation

The gel samples were prepared by base-catalyzed hydrolysis of tetramethoxy-silane (TMOS) in the presence of a large amount of methanol (MeOH). A 0.1 mol/dm^3 aqueous ammonia solution is added dropwise to TMOS under continuous stirring. Both liquids have been mixed previously with an equal volume of methanol. The final mixture contains water and TMOS in a 4:1 molar ratio, which is twice the stoichiometric amount necessary for the formation of SiO_2 from TMOS. The methanol amount was chosen to yield the desired porosity, the compositions can be found in Table 1. TMOS (purum, Fluka), 0.1 mol/dm^3 aqueous ammonia solution (Aldrich) and MeOH (rein, Merck) were used without further purification. TMOS is stored under Ar atmosphere.

Table 1
Volumetric relations of the chemicals needed for the production of SiO_2 gels with desired porosity, scaled linearly when necessary

Porosity, ε (%)	MeOH, V/cm^3	H_2O , V/cm^3	TMOS, V/cm^3
94.0	549.6	144.0	295.2
94.5	587.2	132.0	270.6
95.0	624.7	120.0	246.0
95.5	662.2	108.0	221.4
96.0	699.7	96.0	196.8
96.5	737.3	84.0	172.2
97.0	774.8	72.0	147.6
97.5	812.3	60.0	123.0
98.0	849.8	48.0	98.4
99.0	924.9	24.0	49.2

After mixing, the liquid was left to stand approximately 5 min with continuous stirring. Subsequently, it was filled into containers suitable for the measurements and stored at 22°C (air-conditioning).

The experimentally accessible porosities are restricted by the gelation times. Whereas samples with porosities smaller than 95.5% had to be cooled with a water/ice mixture in order to prevent gelation already in the mixing flask, samples with a porosity of 99% and higher did not solidify within one month. Notice that the ammonia concentration is an important parameter in this respect. The first elastic response of samples with 97.5% porosity appeared after approximately 10 h.

After preparation, the gel samples suffer from methanol evaporation. This can be avoided by a careful sealing of the container, which was not always possible in the present investigation. Alternatively, one may replace the lost methanol, possibly taking provision for the evaporation loss by an excess amount, or cover the gels with an insoluble oil. The latter was avoided in the present study, because the acoustic boundary condition as well as the rheological measurements may be affected in an unknown and irreproducible way. However, an excess amount of methanol may also influence the gel during the aging process, as it could counteract the syneresis or lead to partial swelling.

I refer to Refs. [19] for information about the gel/aerogel structural properties in dependence of the pH during preparation, and to Refs. [20] for information about the structural changes during aging.

3.2. Determination of the gel mass density

For the determination of the gel density, the liquid sample had been filled into polypropene syringes with $(4.67 \pm 0.05) \text{ mm}$ inner diameter, which were efficiently sealed subsequently. After four days, the gel rod was taken out of the syringe and cut into approximately 1 mm long rods; thickness was assumed to be unchanged, strong deviations would have been noticed. The rods were put into air-tight transparent containers. The rod's weight and length were determined using a precision balance (resolution 1 mg) and an inspection microscope, equipped with a translation stage with a micrometer gauge (resolution 0.01 mm). These comparatively coarse resolutions turned out to be sufficient, the main error being the difficult length determination owing to the imperfect cut. The rods suffer from evaporation of methanol, which was noticeable as the surface became increasingly scabby. In order to assure reproducibility, I reversed the order of weighing and length determination twice for three series of density determination. The mass density data that were obtained for these three independent runs are shown in Fig. 1. The dashed line in Fig. 1 follows $\rho = \varepsilon\rho_f + (1 - \varepsilon)\rho_s$, with $\rho_f = 790 \text{ kg/m}^3$ the methanol density, and $\rho_s = 2000 \text{ kg/m}^3$ the skeletal

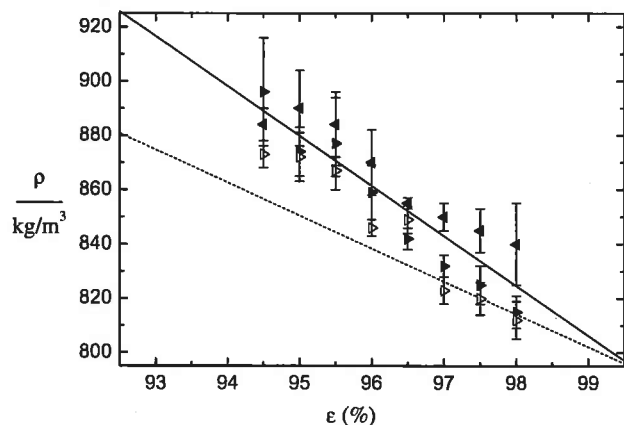


Fig. 1. Mass density ρ of the gels as a function of porosity ε . Three different runs are indicated by different symbols. Triangles pointing right: 94.5→98.0%, length determination first, mass determination subsequently. Triangles pointing left: 98.0→94.5%, weight determination first, length determination subsequently. Drawn lines: see text.

density of the silica frame; this estimate is clearly insufficient to describe the measured mass density as a function of porosity. The solid line has been calculated taking into account the remaining amount of water after a stoichiometric reaction (cf. Section 3.1) with TMOS, and the increased amount of methanol following the reaction. In addition, the density ρ_f of the resulting methanol/water liquid mixture has been calculated taking into account the partial molar volumes of respective compositions, data were taken from the CRC handbook [21]. The experimental data follow this calculation very closely, thus confirming at the same time the relation between the initial sample composition and desired porosity (cf. Table 1).

3.3. Determination of the shear modulus

The viscoelastic properties of the samples were determined using an UDS 200 rheometer (Physica, Stuttgart, Germany) in plate–plate configuration. The complex shear modulus was measured applying a harmonic torsional oscillation of the tool (MP 31, 50 mm diameter) with constant maximal shear stress (10 Pa). The samples were filled into polystyrene dishes (55 mm inner diameter). The lid was sealed with teflon tape after gelation and addition of a layer of 5 mm methanol in excess. The rheological measurements were performed five days after synthesis. The dish was fixed on the lower plate of the rheometer with adhesive tape. After removing the lid, the tool was lowered into the methanol layer under normal force control. The downward movement of the tool was stopped when the normal force exceeded 2.5 N. This limit was established to yield reproducible results by former reference measurements with several gel samples. The normal force relaxes insignificantly afterwards. Linearity of the strain at the maximum stress

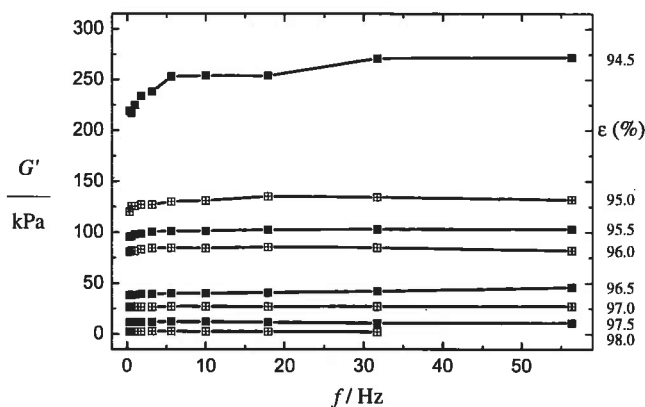


Fig. 2. Real part of the shear modulus G' of the gels as a function of frequency f for different sample porosities ε as indicated to the right. The error of the data points is below 10%, the lines connecting the data points are thought for trend analysis only.

of 10 Pa was checked by repeating the measurement with different stresses (1, ..., 50 Pa) subsequent to every individual measurement. Samples with $\varepsilon = 98\%$ were limited with respect to this linearity to about 30 Hz oscillation frequency. The reproducibility of the measurements was checked by investigating two samples for every given porosity.

The results for the real part G' of the shear modulus (mean of two samples) are shown in Fig. 2. A plateau value in G' is readily observed for every sample porosity. The reproducibility of this plateau value is better than 5%. The imaginary part $G'' \approx 1$ kPa is almost independent of test frequency and sample porosity. Samples with $\varepsilon = 98.0\%$ exhibit a slightly smaller value of G' .

3.4. Determination and evaluation of the acoustical spectrum

The acoustic measurements are quite simple: I used a condenser microphone (EM-4, Conrad Elektronik, Germany), which comes with an internal amplifier and a load resistor within a metal housing (10 mm outer diameter). Power is provided by an external 3-V-battery. The microphone output was AC coupled to the high-impedance input of a digital oscilloscope (9314, LeCroy, USA). The oscilloscope performs a Fast Fourier Transformation using 5000 data points of the signal trace. The Nyquist frequency was 2.5 kHz, resulting in a frequency step of 1 Hz. The applied Hamming window reduces the frequency resolution to 1.4 Hz. 30 FFT sweeps were averaged to yield the final spectrogram.

Samples were contained in cylindrical glass vials with plastic snap-in lids, the inner diameter of the vials was 27 mm. They were filled with four different volumes of gelling liquid, thus leading to four gel cylinders of different height for every given porosity. The acoustical measurements were performed eight days after synthesis. The membrane of the condenser microphone was put into

contact with the glass wall, the vial being held by hand at its plastic lid. The wall was struck with a metallic screw driver. The corresponding pressure pulse is regarded as a white-noise source that excites almost every sound mode within the sample simultaneously, however, possibly with different amplitude, depending on the locus of the point of contact between screw driver and glass cylinder. This was observed experimentally as the increase in signal-to-noise ratio of the sound modes was different for every pulse out of the 30 samples. The oscilloscope is pre-triggered onto the excitement signal with a delay of 0.05s, the time-base being 0.1s. The amplitude of the oscillations, decaying in time, was approximately 5mV, the amplitude of the excitement pulse of the order of 25mV. Pre-trigger and a 20-mV-trigger level assured that the acoustic signal is dominated by the sound modes of the gel and recorded subsequent to a screw driver pulse only.

In order to reduce spurious ambient sound, the spectra are divided by a reference spectrum obtained from a glass vial filled to the same height with water. Besides a strong 50-Hz-contribution, the background noise is at least one order of magnitude smaller in amplitude.

Fig. 3 shows the acoustical spectrum obtained as described above for a representative sample with 97.5% porosity. The vertical thin lines represent the expected resonance frequencies of a cylindrical, homogeneous body with isotropic sound velocity. These can be calculated from the wave equation in cylindrical coordinates r, θ, z , for the particle displacement ξ in the sound field, using a separation ansatz for these coordinates. The general solution reads

$$\xi = \xi_0 \exp(-i\omega t) J_l(k_r r) \cos(l\theta) \cos(k_z z). \quad (4)$$

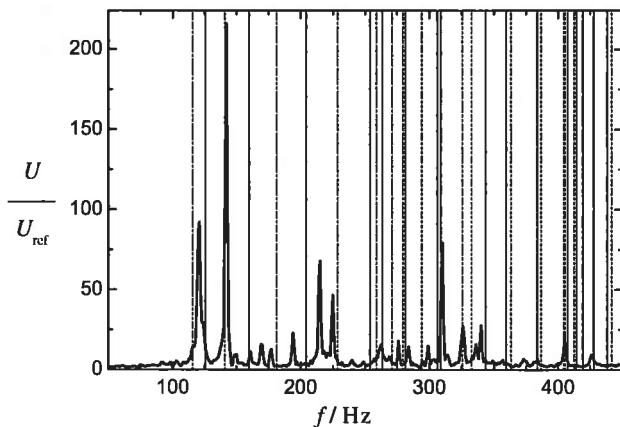


Fig. 3. Normalized sound amplitude U as a function of frequency f for one gel sample with $\varepsilon = 97.5\%$. Expected eigenfrequencies are indicated for few modes: $l = 0, m, n$ even – solid; $l = 0, m, n$ odd – dashed. $f_{011} = 116\text{Hz}$, $f_{111} = 181\text{Hz}$. Parameters for the calculation are $H = 36\text{mm}$, $2R = 28\text{mm}$, and $c_T = 4.1\text{m/s}$. Eigenfrequencies $l > 0$ are omitted for clarity, close to 200Hz are expected $f_{113} = 198\text{Hz}$ and $f_{114} = 212\text{Hz}$.

The resonance frequencies belong to modes with wave vectors given by

$$k^2 = \frac{\omega^2}{c^2} = k_{r,\theta}^2 + k_z^2, \quad (5)$$

which can be specified applying appropriate boundary conditions. The eigenfrequencies for a rod of height H and diameter $2R$ are given by

$$f_{lmn} = \frac{c}{2} \left[\left(\frac{u_{l,m}}{\pi R} \right)^2 + \left(\frac{n}{2H} \right)^2 \right]^{1/2}, \quad (6)$$

where $\omega = 2\pi f$ has been used. $u_{l,m}$ is the m th root of the l th order Bessel function $J_l(k_r r)$. Tabulated values have been taken from Ref. [22]. The use of the $u_{l,m}$ implies acoustically hard walls with a node of the particle displacement in the cylinder's cross-section. This is a good approximation for the glass walls surrounding the gel. However, the situation is less obvious in the z direction, parallel to the axis of the cylinder, as the gel surface may be deformed by the sound wave and the layer of methanol on the surface might have to be taken into account. If the gel surface were an acoustically hard wall, we should observe the selection rule $n = 2, 4, 6, \dots$, meaning that half a wavelength fits into the space between the gel surface and the glass bottom. An acoustically soft surface, however, would imply a quarter-wave fitting into the height of the cylinder, with a wave crest on the gel surface. This would yield the selection rule $n = 1, 3, 5, \dots$

From Fig. 3, we observe that both kinds of modes are present in this experiment. A very formal explanation can be given for this observation, if one calculates the reflection coefficient of the (exponential decaying, $\delta < 0.1\text{mm}$) shear wave at the gel/methanol interface, using the respective impedance $Z = \rho c$. This yields $R = 0.6$, implying that roughly half of the sound intensity experiences the methanol layer on the gel surface as an acoustically hard wall.

Fig. 3 shows a very satisfactory agreement between calculated and experimental frequencies, bearing in mind that only modes with $l = 0$ are drawn for clearness of the plot. The main fitting parameter between the experimental result and Eq. (6) is the sound velocity, which is $c_T = 4.1\text{m/s}$ for this particular sample. In addition, the sample height and width have to be slightly modified ($\approx 1\text{mm}$) as compared to the measured physical dimensions of the sample. This procedure can be justified by the observation that the glass bottom as well as the gel surface are slightly curved and the inner diameter of the glass vials has not been measured for every individual sample. Note that the agreement between measured spectrum and calculation is worse than reported earlier [18]. The difference is most probably due to stress caused by swelling of the gel owing to the excess amount of methanol, which had not been added to the samples earlier.

With decreasing porosity, the satisfactory agreement deteriorates. It is no longer always possible to find a set of parameters where the first few resonance frequencies are located at calculated positions. (Notice that owing to the tremendous number of modes, at higher frequencies this can be remedied easily, but without significance.) At the same time, less individual resonance frequencies and lower sound amplitudes were observed. Whereas the latter two observations may be readily explained by the increasing stiffness of the gel, the former observation merits a further comment later.

The evaluation of the spectrum benefits from the linear relationship between acoustic pressure and signal voltage, because no beat frequencies, sum frequencies, or harmonics are generated by the detector. The frequency response of the condenser microphone used is constant between 20 Hz and 18 kHz.

4. Results and discussion

To determine the sound velocity from the acoustic spectra, the procedure as described in the previous chapter turned out to be too lengthy, and the detailed information (mode assignment and frequency) as not necessary. Therefore, I adopted a simpler approach.

The first visible resonance in the spectra (whatever its amplitude is), is assumed to be the fundamental mode f_{011} . In order to check this assumption, the respective frequencies for different cylinder heights are fitted to a common curve given by Eq. (6), with $u_{0,1} \approx 2.405$ and $n = 1$. The result is shown in Fig. 4 for the samples under study, the sound velocity is the only fit parameter. Missing samples were destroyed during the measurements. In general, good agreement between measurement and prediction is observed. Again, the agreement deteriorates

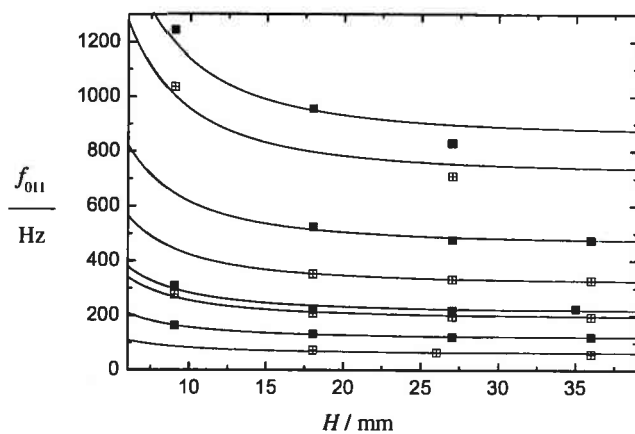


Fig. 4. Fundamental sound mode frequency f_{011} as a function of cylinder height H for different gel samples. A fit to the theoretical expression (solid lines, see text) was used to determine the sound velocity c_T . Sample porosity increases from top to bottom from 94.5% to 98% as in Fig. 2.

with decreasing porosity and, correspondingly, increasing acoustic frequencies.

With decreasing porosity, naturally, the volume of the skeleton material increases at the expense of the liquid volume, leading to an increase of the mass density of the porous body (cf. Fig. 1). The shear modulus, however, increases at the same time by one or two orders of magnitude (cf. Fig. 2), indicating that not only the walls become thicker, but also the link density between the walls increases. In accordance with Eq. (3), this should lead to an increase in transversal sound velocity.

The corresponding data are shown in Fig. 5, which confirms this expectation. The open squares stand for the sound velocity calculated according to Eq. (3), using the plateau value of the shear modulus determined from Fig. 2 and the respective mass density from Fig. 1. A linear fit to the calculated data is shown as well, together with a 95% confidence band. The solid circles are the sound velocities as obtained from the acoustical measurements represented by the data shown in Fig. 4.

Excellent agreement between calculated and measured data for the transversal sound velocity between $\varepsilon = 96\%$ and 98% is observed. There is no fit parameter, and I regard this close agreement between acoustical measurement and rheological prediction as the desired evidence that the audible sound generation from the gels originates from resonances of the shear waves within the gel body.

Below $\varepsilon = 96\%$, the data deviate increasingly. From Fig. 4, it can be read that every resonance frequency within these gels is higher than approximately 500 Hz. Fig. 2 shows that the rheometer can determine strain data in a linear fashion up to approximately 60 Hz only. Correspondingly, I attribute the increasing deviation of

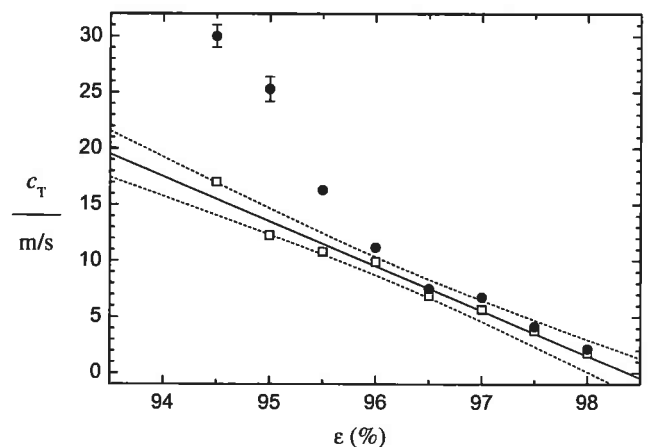


Fig. 5. Transversal sound velocity c_T as a function of gel sample porosity ε . (\square) Calculated values, using the plateau modulus G' and the mass density ρ ; a linear fit to these data (—) and a 95% confidence band (---) are also plotted. (\bullet) Experimental acoustic resonance data as obtained from Fig. 4. Error bars are drawn if larger than the symbol.

the acoustical and rheological data to an increase of the shear modulus with frequency. A plot according to Fig. 2 drawn for higher frequencies would no longer show a plateau, but a shear modulus increasing with frequency. Unfortunately, this assumption cannot be verified within the scope of the present contribution. On the other hand, if this explanation could be confirmed, it would allow the application of acoustic measurements as presented in this contribution for the determination of shear moduli at higher frequencies.

At the same time, this observation explains why samples with low porosity exhibit stronger deviations between observed resonance frequencies and calculated eigenmodes. As the sound velocity is no longer a simple parameter, but frequency dependent, the calculation of the spectra gets prohibitively complicated. Note that the dispersion is non-linear (cf. Eq. (3)).

In conclusion let me stress that this paper gives, for the first time, an explanation for the strange humming observed in some kind of gels. The audible emission originates from a resonance of shear modes within the gel body. If the shear moduli were known in advance, this finding would allow the assembly of a gel xylophone by using gel cylinders of appropriate height and porosity. In addition, the effect could eventually be applied for the determination of shear moduli at frequencies where no conventional rheometer is available.

Acknowledgments

The experimental part of this work was performed during my research visit at the IAP of the University of Bern, Switzerland. I gratefully acknowledge the stimulating and pleasant collaboration with T. Binkert, G. Bucher, I. Flammer, and J. Rička. The rheological measurements were performed with the group of P. Schurtenberger at the Université de Fribourg, Switzerland, to whom I thank for his support. C. Sommer helped a lot in performing the measurements. A. Emmerling, University of Würzburg, Germany, provided me with the gel recipes that lead to Table 1. This work has been financed by a research scholarship of Deutsche Forschungsgemeinschaft and the Swiss National Foundation.

References

- [1] M.A. Boit, *J. Appl. Phys.* 33 (1962) 1482; *J. Acoust. Soc. Amer.* 34 (1962) 1254.
- [2] P.R. Ogushwitz, *J. Acoust. Soc. Amer.* 77 (1985) 429.
- [3] P.R. Ogushwitz, *J. Acoust. Soc. Amer.* 77 (1985) 441; J.M. Hovem, *J. Acoust. Soc. Amer.* 67 (1980) 1559, 68 (1980) 1531 (erratum).
- [4] A. Golov, D.A. Geller, J.M. Parpia, N. Mulders, *Phys. Rev. Lett.* 82 (1999) 3492.
- [5] D.L. Johnson, *J. Chem. Phys.* 77 (1982) 1531.
- [6] T.J. Plona, D.L. Johnson, in: D.L. Johnson, P.N. Sen (Eds.), *Physics and Chemistry of Porous Media*, AIP, New York, 1984, p. 89.
- [7] T. Bourbié, O. Coussy, B. Zinszner, *Acoustics of Porous Media*, Éditions Technip, Paris, 1987.
- [8] A.W. Wood, *A Textbook of Sound*, MacMillan, New York, 1941.
- [9] L.D. Landau, E.M. Lifshitz, *Lehrbuch der Theoretischen Physik*, Band VI: Hydrodynamik, Akademie, Berlin, 1991.
- [10] T. Tanaka, L.O. Hocker, G.B. Benedek, *J. Chem. Phys.* 59 (1973) 5151.
- [11] M. Kimura, T. Ishikawa, S. Kawashima, *Jpn. J. Appl. Phys.* 37 (1998) 3152; A.K. Holmes, R.E. Challis, *Langmuir* 15 (1999) 3045; D.O. Riese, G.H. Wegdam, *Phys. Rev. Lett.* 82 (1999) 1676.
- [12] J.C. Bacri, J. Dumas, A. Levelut, *J. Phys. France Lett.* 40 (1979) L-231; S.C. Ng, Y. Li, *J. Phys. II France* 3 (1993) 1241.
- [13] M. Gronauer, J. Fricke, *Acoustica* 59 (1986) 177; J. Gross, J. Fricke, *J. Non-Cryst. Solids* 145 (1992) 217.
- [14] J. Gross, G.W. Scherer, C.T. Alviso, R.W. Pekala, *J. Non-Cryst. Solids* 211 (1997) 132; L. Forest, V. Gibiat, T. Woignier, *J. Non-Cryst. Solids* 225 (1998) 287; *Ultrasonics* 36 (1998) 477.
- [15] M. Gradzielski, H. Hoffmann, G. Oetter, *Colloid Polym. Sci.* 268 (1990) 167.
- [16] G. Oetter, H. Hoffmann, *Colloids Surf. A* 38 (1989) 225.
- [17] F. Kohlrausch, *Z. Phys. Chem.* 12 (1893) 773.
- [18] C. Sinn, *Progr. Colloid Polym. Sci.* 115 (2000) 325.
- [19] C.J. Brinker, G.W. Scherer, *J. Non-Cryst. Solids* 70 (1985) 301; J. Pelous, M. Foret, R. Vacher, *J. Non-Cryst. Solids* 145 (1992) 63; A. Emmerling, J. Fricke, *J. Non-Cryst. Solids* 145 (1992) 113.
- [20] H. Hdach, T. Woignier, J. Phalippou, G.W. Scherer, *J. Non-Cryst. Solids* 121 (1990) 202; P.J. Davis, C.J. Brinker, D.M. Smith, *J. Non-Cryst. Solids* 142 (1992) 189.
- [21] R.C. Weast (Ed.), *CRC Handbook of Chemistry and Physics*, 64th Ed., CRC, Boca Raton, 1983 (table D-242).
- [22] M. Abramowitz, I.A. Stegun, *Handbook of Mathematical Functions*, Dover, New York, 1970.